Next Generation Ultrafiltration for Wastewater Treatment

Characterization and Performance of Fouling-Resistant Polymeric and Lyocell Cellulose Nanofiber Membranes

RIYA PATEL

INTRODUCTION

Providing sustainable and affordable clean water to the four billion people in developing nations that are expected to face water shortages by 2050 is an imperative goal [1-5]. Imminent global water scarcities are increasing demand for alternative water sources, such as reclaimed wastewater [6-12]. Membrane technology, specifically ultrafiltration, is a key component of wastewater reclamation due to its separation efficiency, minimal energy consumption, and economic feasibility [13-16]. Thin film nanocomposite ultrafiltration membranes comprise of three layers: a supporting substrate, a mid-layer scaffold, and a thin top coating (Figure 1). Modifications to polymeric ultrafiltration scaffolds have enhanced traditional wastewater treatment since membrane efficiency heavily depends on membrane characteristics [17-19].

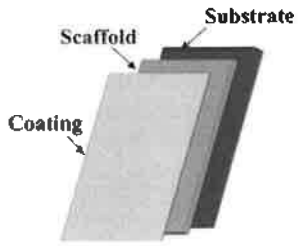

Figure 1. Thin Film Nanocomposite Membrane Structure.

Currently, modified polymer membrane scaffolds, such as polyvinylidene fluoride (PVDF), polyacrylonitrile (PAN), and polyethersulfone (PES), are fabricated through electrospinning to enhance porosity, surface area to volume ratio, and permeability [20-22]. However, electrospun polymer ultrafiltration scaffold applications are deterred by two major obstacles: electrospun scaffolds are 1) susceptible to fouling caused by surface hydrophobicity and electrostatic adhesion to foulants [23, 24] and 2) environmentally and economically unsustainable due to non-biodegradability and resource-intensive manufacturing [25, 26].

Membrane fouling is characterized by undesirable accumulation and deposition of particles on or within membrane pores, often caused by physical and chemical interactions among membranes and foulants [27-29]. Membrane fouling results in decreased membrane performance and lifetime, increased operating costs and physical or chemical maintenance requirements [30-33]. Membrane fouling control can be achieved through the adjustment of operating conditions and membrane modifications, both functional techniques to enhance membrane performance [34-36]. Operating conditions, including transmembrane pressure, filtration temperature, and module configuration, are easily adjustable membrane fouling control techniques [37]. Membrane modifications include pre-treatments (facile coatings with hydrophilic additives) [38-40], or post-treatments (plasma and electron irradiation) [41, 42]. Membrane coating techniques increase

membrane hydrophilicity and therefore reduce fouling by weakening attractions between foulants and the membrane surface [43-48].

A commonly used pre-treatment membrane coating is cellulose nanofibers (CNF). CNF's favorable characteristics include fibrous nature, distinctive mechanical properties, low cost, sustainability, and abundance. CNF membrane coatings improve fouling resistance for wastewater reclamation due to its inherent hydrophilicity [49]. CNF hydrophilicity is directly correlated with the high density of negatively charged hydroxyl and carboxyl groups [50]. Further enhancement of hydrophilicity of CNF is commonly achieved through the highly selective and energy-efficient 2,2,6,6-tetramethylpiperidine-1-oxyl radical-mediated (TEMPO) oxidation process [51], where C_6 primary hydroxyl groups are oxidized to carboxyl groups increasing the density of negative charges [52]. Recently, TEMPO-oxidized CNF coatings on fouling-susceptible electrospun scaffolds have demonstrated outstanding flux (due to high porosity of the scaffold) and fouling resistance [53-55]. The CNF-layer thickness and surface charge are vital membrane characteristics that influence hydrophilicity and fouling-resistance [56, 57]; however, determining optimal CNF-layer thickness and surface charge for fouling resistance of electrospun ultrafiltration membranes is unstudied.

CNF-layer thickness is a significant variable to membrane fouling behavior. Thicker CNF-layers generally tend to have low flux because water molecules require more time to filter through the coating later. However, increasing CNF thickness may result in improved fouling resistance, due to higher density of negatively charged functional groups leading to stronger repulsive forces (Figure 2) [58-60]. Finding an optimal membrane thickness to balance flux and fouling resistance is crucial for efficient membrane operation.

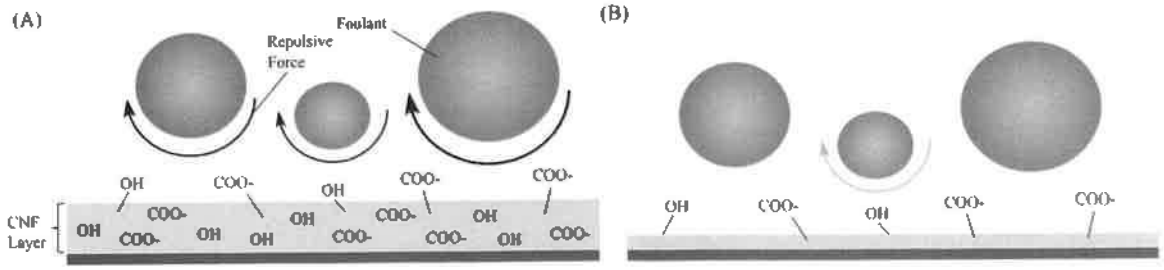

Figure 2. CNF-Layer Thickness on Electrostatic Repulsions with Foulants. Greater density of negative hydroxyl and carboxyl groups are present in the (A) higher thickness (>100nm) than the (B) lower thickness (<100nm) predicting less fouling.

Charge interactions between a membrane and foulants are crucial variables in decreasing membrane fouling [36, 61]. When CNF membrane surfaces and foulants share similar charges, strong repulsive forces exist, thereby decreasing foulant accumulation on the membrane surface (Figure 3) [62]. Surface charges can be altered through facile modifications, such as increasing concentrations of oxidizing agents (NaClO/NaBrO) in CNF TEMPO-oxidation [63-65].

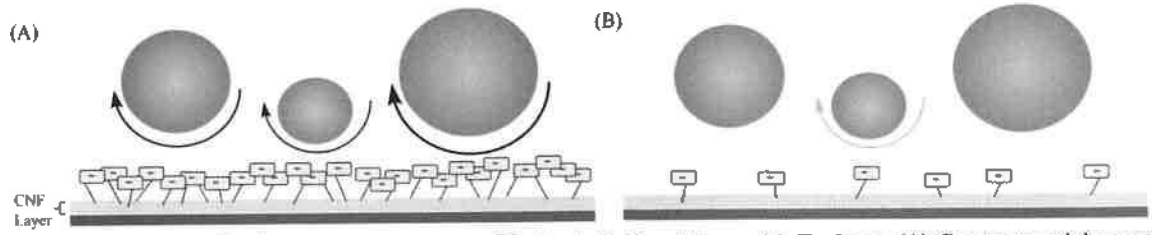

Figure 3. CNF-Layer Surface Charge Density on Electrostatic Repulsions with Foulants. (A) Greater negativity results in repulsions with negatively charged foulants than the (B) less negative membrane, thus greater surface charge is predicted to decrease fouling.

To address the second limitation– environmental and economic unsustainability– of current electrospun polymeric membranes, lyocell has been introduced as a regenerated cellulose fiber extracted from wood pulp currently applied in the textile industry. However, it has exhibited promise as an alternative ultrafiltration scaffold due to its biodegradability, simplistic synthesis (dissolution in N-methyl morpholine-N-oxide, a cheap and non-toxic fiber solvent), superior hydrophilicity, remarkable mechanical fiber properties, and benign economic and environmental impact [66, 67].

Thin film nanocomposite membranes prepared in this study consisted of three layers: a polyethylene terephthalate supporting substrate, a scaffolding porous mid-layer comprising of either electrospun polyacrylonitrile (ePAN) or lyocell, and a hydrophilic TEMPO-oxidized CNF coating consisting of variable thickness and surface charges.

PURPOSE

This study aims to clarify antifouling properties of electrospun scaffolds as well as introduce alternatives to current ultrafiltration membranes for wastewater reclamation by 1) characterizing morphology and determining fouling-resistant behavior of CNF ePAN membranes' thicknesses; 2) characterizing ePAN membranes' surface charges pre- and post- fouling and elucidating antifouling filtration performance; 3) comparing performance of a novel lyocell scaffold to CNF coated ePAN scaffolds and commercial membrane and characterizing the lyocell

membranes, PVDFA6; 4) computationally deriving Hermia's fouling model values for ePAN and lyocell membranes; and 5) determining fouling-resistant performance of an all-cellulose lyocell-CNF mixture membrane.

EXPERIMENTAL

Materials

TEMPO-oxidized CNF fibers and ePAN scaffolds were prepared according to Hadi et al. [68]. Lyocell fibers were suspended in a 0.5 weight percent (wt%) suspension and mixed for 24 hours (EFTec Nanofibrillated Lyocell Fiber, Engineered Fibers Technology, Shelton CT). Commercial ultrafiltration membrane, PVDFA6, was purchased from Sterlitech Corporation (Lot # 072617R3, Synder Filtration, Vacaville, California).

Membrane Preparation

The ePAN scaffolds were coated with CNF of varying thicknesses and degrees of oxidation. Area density (AD), a quantitative measure of thickness, was determined through different coatings of 0.15 wt% CNF suspension on the ePAN scaffold. Degrees of oxidation (DO), a quantitative measure of surface charge density, were produced through CNF TEMPO-oxidation and were previously measured through conductometric titrations [62]. For lyocell membranes, 0.5 wt% lyocell suspension was poured into a large ceramic funnel, filtered overnight, dried for 3 hours at 50°C, coated with 0.15 wt% CNF suspension, crosslinked with 0.5 wt% polyacrylate emulsions (PAE; Solines, Wilmington, DE, USA), and cured at 120°C for 20 minutes.

Operating Pressure

A dead-end fouling test with an active filtration area of 0.00146 m^2 was conducted at 7 or 17 psi, using compressed nitrogen gas, to determine optimal operating pressures of CNF coated ePAN membranes (Sterlitech Co. Dead End Device, HP4750 Stir Cell, Kent, USA). Each membrane was initially compacted with distilled water (250 mL) to measure pure water flux, then fouled with wastewater (250mL), obtained from Riverhead Sewage Treatment Plant (Riverhead, NY), in one-hour cycles. Between each cycle, the membrane was transferred out of the dead-end cell and cleaned with a 10 second distilled water flush. Flux was calculated by recording permeate

mass and operating pressure in one-minute increments over four cycles and using Eq. 1

$$J = \frac{V}{A\Delta t} \quad (1)$$

where J is flux, V is permeate volume (L), A is membrane area (m^2) and Δt is time interval (h).

Flux recovery ratios were calculated after hydraulic cleaning and calculated using Eq. 2

$$Flux\ Recovery = \frac{J_f}{J_0}\ x\ 100 \quad (2)$$

where J_0 is flux immediately after membrane cleaning and J_f is flux after the fouling cycle measured in $L \cdot m^{-2} \cdot h^{-1}$ (LMH). This dead-end fouling procedure was repeated for all membrane filtration performance experiments.

Area Density (AD)

Focused ion beam-scanning electron microscopy (FIB-SEM, crossbeam 340; Carl Zeiss Microscopy, LLC) was performed on cross-sections of pristine 0.22 and 0.40 AD ePAN membranes to determine CNF coating thickness. Dead-end filtration wasconducted to elucidate fouling behavior at 0.22 and 0.40 AD CNF thicknesses.

Degree of Oxidation (DO)

Surface charge densities of 1.80 DO and 1.35 DO ePAN membranes and sludge samples, the solid form of wastewater, were determined via zeta potential analyses with Electrokinetic Analyzer for Solid Surface Analysis (Anton Paar, SurPASS 3) at pH 7 and 1 mM KCl as the electrolyte solution. Membranes were placed on a 20×10 mm gap cell with a gap distance of approximately 115 μm. To determine DO's impact on fouling behavior of ePAN membranes, dead-end filtration was carried out with 1.80 DO and 1.35 DO membranes and flux recovery was calculated. Fourier transform infrared spectroscopy (FTIR) and water contact angles tests were performed on pristine and fouled 1.80 DO and 1.35 DO ePAN membranes to attribute differences in fouling to crosslinking and hydrophilicity, respectively. FTIR in attenuated total reflectance mode was performed on ePAN membranes and sludge samples to determine crosslinking patterns

(FTIR Spectrometer, Nicolet™ iS™ 10). The spectra were recorded between F. A comparison of hydrophilicity between fouled ePAN membranes at 1.80 DO and 1.35 DO was conducted through a water contact angle goniometer (OCA 15 EC, DataPhysics). A glass syringe (0.52 mm diameter) released a 2.5 μL droplet of distilled water at a dosing rate of 0.2 μL/s, a digital camera recorded the droplet for 30 seconds, and SCA 20 DataPhysics software calculated water contact angle.

Membrane Scaffold

Dead-end filtration with the most fouling-resistant ePAN membrane, lyocell membrane, and PVDFA6 membrane was conducted to introduce and compare lyocell's efficacy as an alternative ultrafiltration scaffold. FTIR and water contact angle experiments were conducted on the fouled lyocell membrane to attribute antifouling to crosslinking and hydrophilicity. Turbidity of the CNF coated ePAN and lyocell membranes was determined using a turbidimeter (Thermo Scientific™ Orion™ AQ4500) in order to determine permeate quality and classify them under government regulations. Then, a GitHub dead-end Hermia's fouling model repository was downloaded on Jupyter Notebook, v. 5.5.0, on Anaconda Navigator, v.1.8.7 to computationally derive Hermia's fouling model values [35]. Hermia's fouling models are commonly applied standardized mathematical models to represent types and degrees of fouling. The computational fouling repository distinguished between complete pore blocking (Figure 4A), intermediate pore blocking (Figure 4B), standard pore blocking (Figure 4C), or cake layer formation (Figure 4D) [69-71]. Time and flux values for 0.40AD 1.80 DO CNF coated ePAN and CNF coated lyocell were inputted to obtain Hermia's fouling model values.

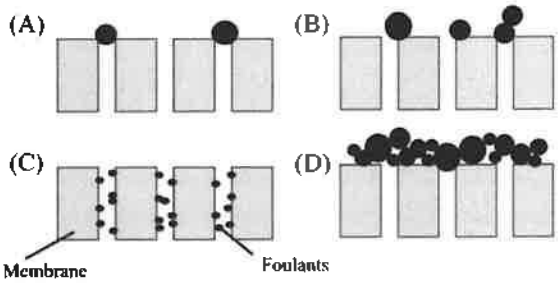

Figure 4. Hermia's Fouling Models. (A) Complete pore blocking, (B) Intermediate pore blocking, (C) Standard pore blocking, (D) Cake layer formation.

All-Cellulose Membrane

Dead-end filtration of the all-cellulose lyocell-CNF mixture membrane was conducted and flux recovery was calculated.

Data Analysis

Standard deviation was calculated for CNF thickness, zeta potential, and water contact angle in Microsoft Excel.

RESULTS AND DISCUSSION

CNF coated membranes were prepared to determine ideal antifouling conditions (ADs, DOs, and scaffold type), characterize membranes pre- and post-fouling, and determine Hermia's fouling models values.

Optimal Operating Pressure

The ePAN membrane at 0.22 AD 1.80 DO was tested in a dead-end cell under two operating pressures: 7 psi and 17 psi (Figure 5). Although there was a higher flux under 17 psi (180 LMH), a greater degree of fouling was observed, demonstrated by low flux recovery (76%). The 7 psi membrane's recovery rate was 82% thus exhibiting reduced fouling when compared to 17 psi. Increased pressures result in further accumulation of foulants on and within membrane pores. Lower pressures are ideal for long term antifouling properties, therefore 7psi was used for all dead-end fouling tests forthgoing.

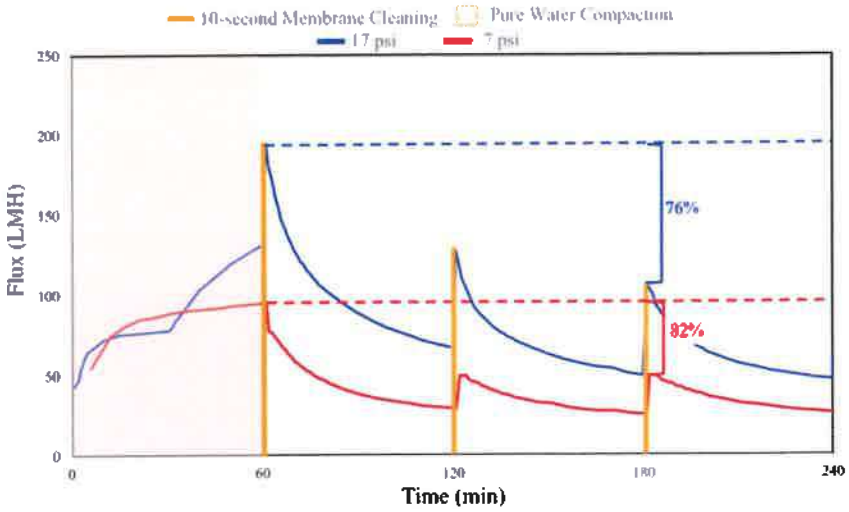

Figure 5. Dead-end fouling of 0.22 AD 1.80 DO CNF Coated ePAN membranes at Various Operating Pressures. The 0.22AD 1.80 DO membranes under 7 psi had the greatest flux recovery using the Sterlitech Co. Dead End Cell.

Area Density (AD)

To determine CNF-layer thickness of varying area density (AD) pristine ePAN membranes, SEM imaging was conducted (Figure 6). Morphology of 0.22 AD and 0.40 AD ePAN membranes demonstrated a CNF-layer thickness of 47.0 ± 18.4 nm for 0.22 AD and 274.5 ± 21.2 nm for 0.40 AD, respectively. CNF thickness per given area correlates with AD and is predictive of enhanced antifouling properties, considering the greater density of negatively charged hydroxyl and carboxyl exposed to the foulants. AD is a necessary characterization to enhance fouling resistance and membrane efficiency.

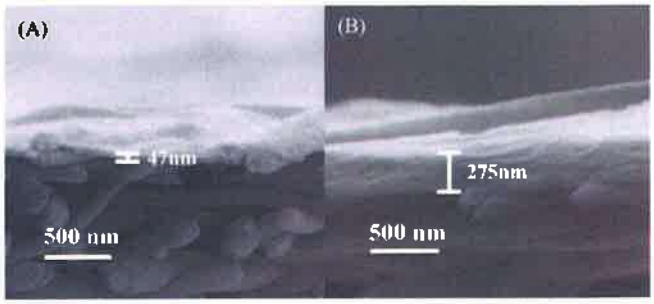

Figure 6. SEM images of (A) 0.22 AD and (B) 0.40 AD CNF coated ePAN. Cross-sections of ePAN membranes were imaged to exhibit the thicker CNF-layer on the 0.40 AD membrane.

The 0.40 and 0.22 AD ePAN membranes' filtration performances were tested via dead-end filtration (Figure 7). The 0.22 AD membrane exhibited a 94 LMH flux initially but fouled rapidly, demonstrated by low recovery rate (63%).

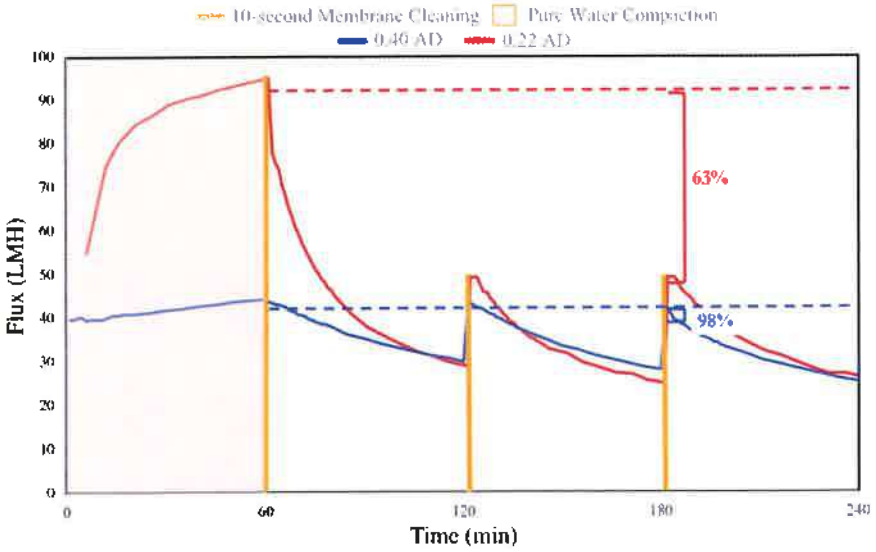

Figure 7. Dead-end fouling of 0.22 AD and 0.40 AD CNF Coated ePAN membranes. The 0.40 AD membrane had a greater flux recovery using Sterlitech Co. Dead End Cell.

The 0.40 AD membrane had a lower initial flux (40 LMH) but exhibited superior flux recovery (98%). Fouling resistance is correlated with density of negatively charged hydroxyl and carboxyl groups that enhance membrane hydrophilicity. Hence, thicker membranes are optimal for antifouling properties.

Degree of Oxidation (DO)

Surface charge density, measured with DO, is an indicator of electrostatic repulsions between membranes and foulants as well as optimal antifouling properties. Due to the negative charge of tested sludge (-12.6 ± 2.0 V), greater negativity of the membrane surface would demonstrate stronger repulsive forces with foulants, leading to decreased fouling. Here, zeta potential was used to estimate the surface charge density of 1.80 DO ePAN membrane (50.0 ± 1.4 V) and 1.35 DO ePAN membrane (-44.2 ± 2.2 V; Figure 8). Since 1.80 DO ePAN had a lower zeta potential, it is anticipated that 1.80 DO will minimize fouling. However, filtration performance comparisons are required to comprehend the relation between DO and fouling resistance.

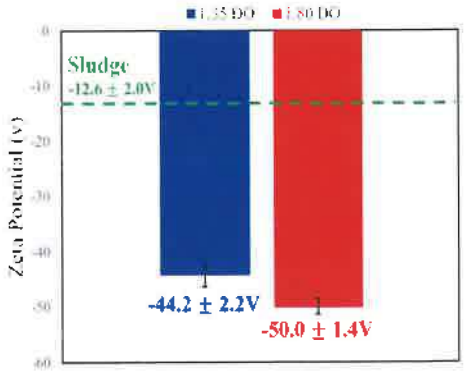

Figure 8. Zeta Potential of CNF coated ePAN at 1.80 DO, 1.35 DO, and sludge. Electrokinetic Analyzer for Solid Surface Analysis: SurPASS™ 3 by Anton Paar used to determine that 1.80 DO exhibited greater surface negativity. Y- error bars denote standard deviation.

A dead-end filtration test was conducted on 1.80 DO and 1.35 DO ePAN membranes to determine the result of varying surface charge on antifouling dynamics (Figure 9A). The 1.35 DO

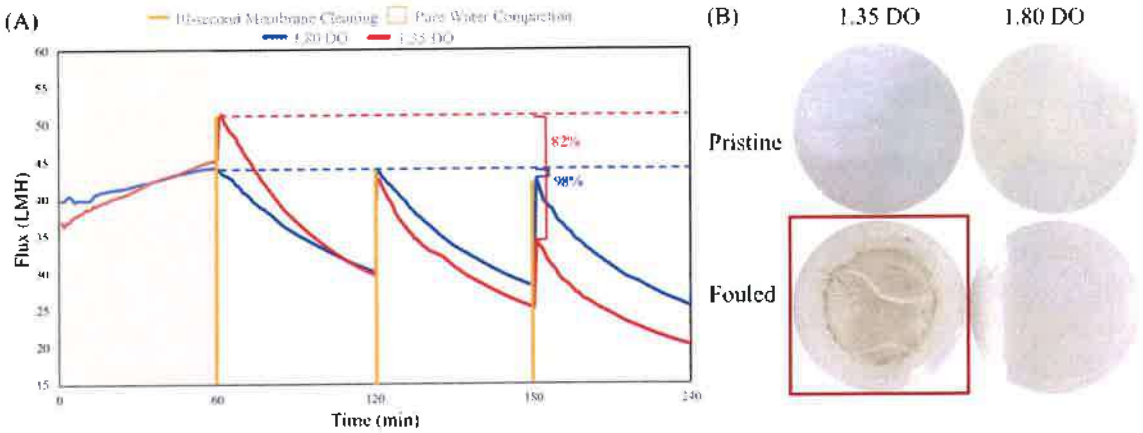

Figure 9. (A) Dead-end fouling and (B) Membrane Photography of 1.80 and 1.35 DO ePAN membranes (pristine and post-filtration). The 1.80 DO membrane had a greater flux recovery using the Sterlitech Co. Dead End Cell. The 1.80 DO membrane had no visual caking since it was flushed away whereas the 1.35 DO membrane a visible cake layer even after hydraulic cleaning.

ePAN had a 51 LMH initial flux, but after 120 minutes, flux had declined rapidly exhibiting a stronger degree of fouling. The 1.80 DO membrane had a flux recovery of 98% and a higher flux after 4 fouling cycles. Membrane photography exhibited a visible cake layer on the 1.35 DO fouled

membrane, but caking on the 1.80 DO fouled membrane was absent (Figure 9B). The non-existent cake layer and high flux recovery rate of the 1.80 DO membrane may be attributed to increased hydrophilicity caused by TEMPO-oxidation of the negatively charged functional groups on CNF. Higher DOs maximize fouling resistance of CNF membranes for wastewater reclamation.

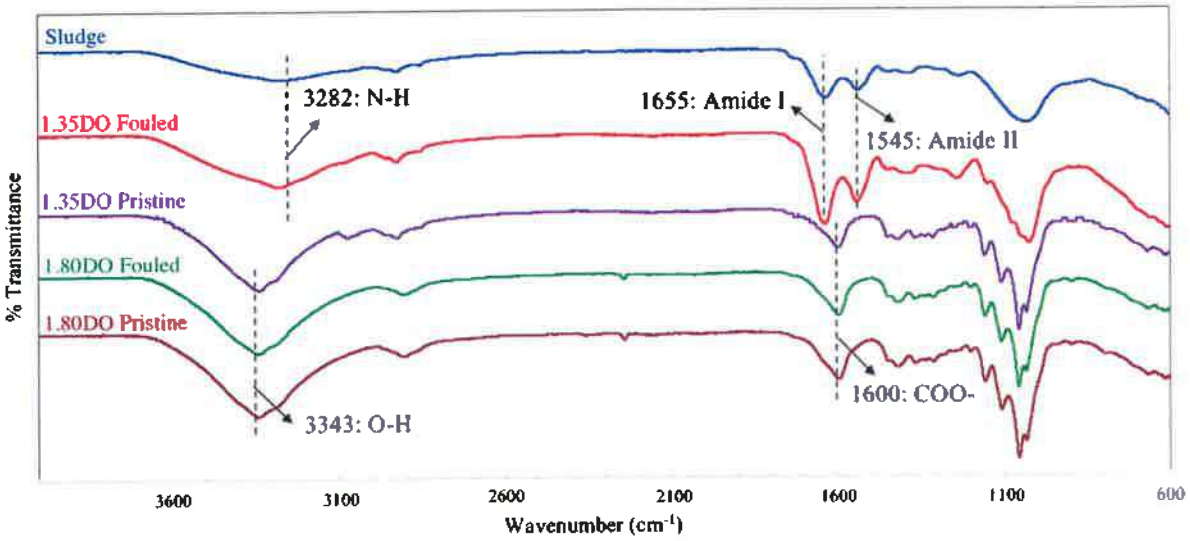

Figure 10. Fourier-transform infrared spectroscopy (FTIR) of pristine and fouled 0.40 AD CNF coated ePAN membranes at 1.80 and 1.35 DO. Using Nicolet™ iS™ 10 FTIR Spectrometer, DO was a vital factor in determining the degree of fouling highlighted by differences in crosslinking of pristine and fouled membranes.

To support the superior fouling resistance of the 1.80 DO ePAN membrane, FTIR and water contact angle tests were conducted to establish crosslinking and hydrophilicity, respectively. FTIR was performed on the test sludge sample, 1.80 DO (pristine and fouled) and 1.35 DO (pristine and fouled) membranes (Figure 10). The fouled 1.35 DO membrane and sludge sample shared amine, amide I and amide II peaks at 3283 cm^{-1}, 1655 cm^{-1} and 1545 cm^{-1}, respectively [72-75]. The fouled 1.80 DO membrane had similar peaks to pristine membranes at hydroxyl and carboxylic acid group peaks at 3343 cm^{-1} and 1600 cm^{-1}, respectively [76-78]. Similar peaks between fouled 1.80 DO membrane and pristine membranes were observed, while the fouled 1.35 DO closely resembled sludge. The presence of amide groups (protein fouling) and N-H group (polysaccharide fouling) on fouled 1.35 DO membrane indicate that irreversible fouling occurred during filtration. Absent fouling peaks on the fouled 1.80 DO membrane support stronger electrostatic repulsions between 1.80 DO membrane and foulants and minimal foulant build up.

Decreasing water contact angles of fouled 1.80 DO and 1.35 DO membranes were compared to highlight differences in hydrophilicity (Figure 11). The 1.80 DO membrane's contact angle decreased 64° over 30 seconds having a 2.13° decline every second. The 1.35 DO membrane only had a contact angle decrease of 15° demonstrating a minimal decrease of 0.516° per second. Considering contact angles above 90° indicate hydrophobicity and sludge is comprised of mostly hydrophobic components [79-83], the 1.35 DO membrane was confirmed to have a greater cake layer. Hydrophobicity decreases antifouling properties of a membrane thus supporting the lower flux recovery of the 1.35 DO membrane compared to 1.80 DO. FTIR and water contact angle were verifying tests that 1.80 DO was more fouling resistant and both crosslinking and hydrophilicity are critical factors in fouling resistance.

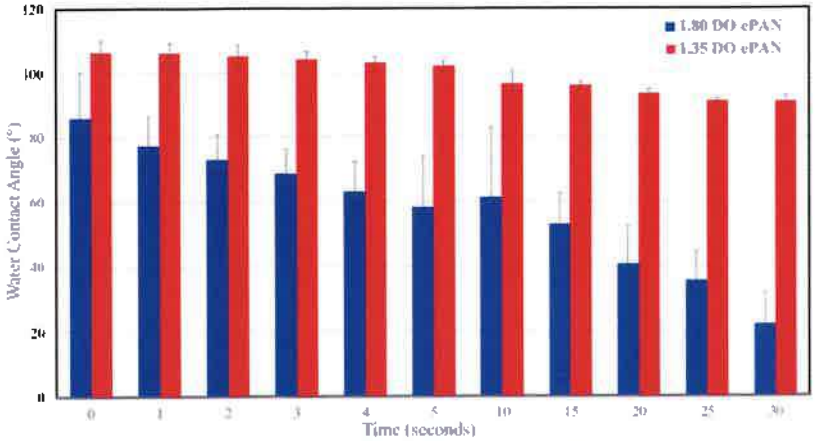

Figure 11. Water Contact Angle of Fouled 1.80 and 1.35 DO ePAN membranes at 0.40AD CNF. Using Data Physics OCA 15EC contact angle goniometer, DO was demonstrated to be a crucial factor in hydrophilicity and antifouling properties of the membrane.

Alternative Membrane Scaffolds

Lyocell is an affordable and environmentally viable substitute for commercial ePAN scaffolds. To test membrane efficacy based upon flux recovery, the CNF coated ePAN with greatest fouling-resistance (0.40 AD 1.80 DO under 7 psi) was compared to CNF coated lyocell and commercial

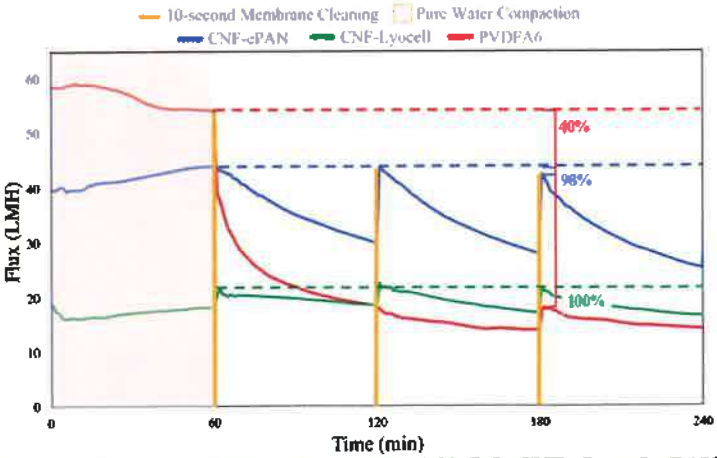

Figure 12. Dead-end fouling of 0.40 AD 1.80 DO CNF Coated ePAN membrane, 0.40AD 1.80 CNF coated Lyocell membrane and commercial membrane, Polyvinylidene fluoride A6 (PVDFA6). The Sterlitech Co. Dead End Cell revealed that the lyocell membrane had the greatest flux recovery.

membrane PVDFA6 (Figure 12). The lyocell membrane had a flux recovery of 100%, however, a lower flux (19 LMH) compared to the ePAN membrane (44 LMH). The remarkable antifouling dynamics of the lyocell membrane highlights lyocell as a superior alternative to currently available polymeric scaffolds, such as ePAN. Overall, both CNF coated membranes presented enhanced flux recovery in comparison to commercial membrane, PVDFA6. Fouling-resistance of CNF coated membranes demonstrates CNF hydrophilicity as an effective mitigator to costly and commercial fouling-susceptible membranes.

The fouling peaks that are shared by the ePAN membrane and the sludge sample are absent on the lyocell membrane as indicated at wavenumbers 3282, 1655, 1545 cm^{-1} (Fig 13). Since the lyocell membrane remained in the pristine state even after the wastewater fouling cycles, its antifouling properties can be supported through crosslinking.

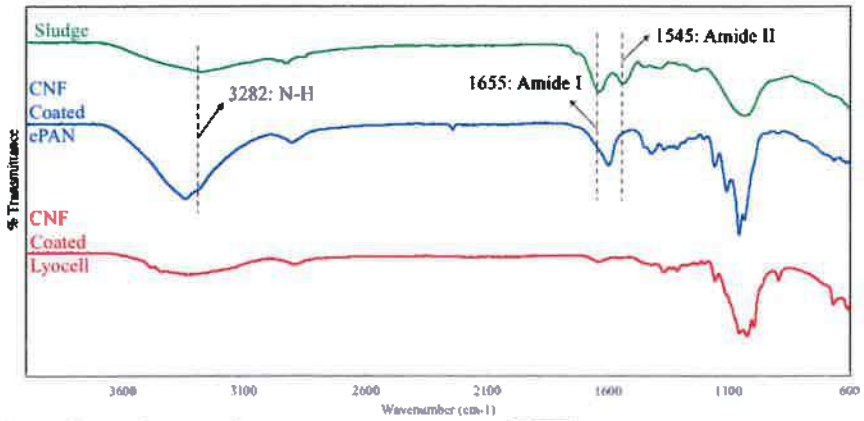

Figure 13. Fourier-transform infrared spectroscopy (FTIR) of fouled 0.40 AD 1.80 DO CNF coated ePAN membrane, CNF coated lyocell membrane and sludge sample. Using Nicolet™ iS™ 10 FTIR Spectrometer, lyocell's absence of fouling peaks indicate low degree of fouling confirmed through crosslinking.

Enhanced hydrophilicity is observed with the lyocell membrane since the water contact angle decreased 83° averaging a 2.76° decline per second. The ePAN membrane only decreased 63°, within 30 seconds, having a decline of 2.13° per second (Fig 14). The greater hydrophilicity of the

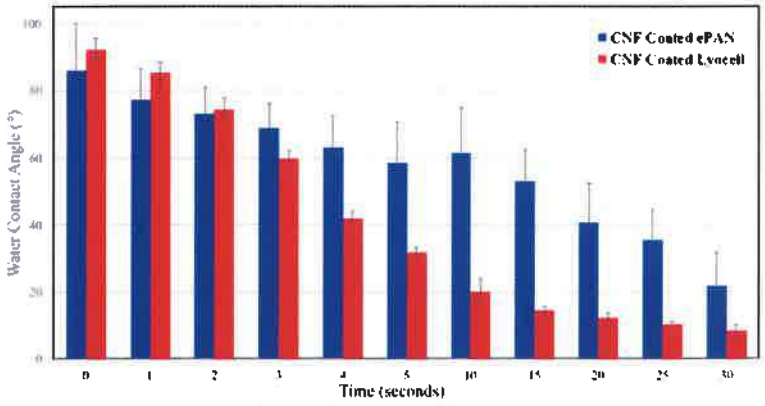

Figure 14. Water Contact Angle of Fouled 0.40 AD 1.80 DO ePAN membrane and CNF coated lyocell membrane. Using Data Physics OCA 15EC contact angle goniometer, increased hydrophilicity of the lyocell membrane supports greater antifouling dynamics.

lyocell membrane indicates support of the greater antifouling properties and thus enhanced membrane performance.

A computational derivation of Hermia's fouling models was completed through a modified Jupyter Notebook program for CNF coated ePAN, CNF coated lyocell, and PVDF to determine the most significant mechanism of fouling (Figure 15). For all membranes, cake layer formation was the primary fouling model. However, cake formation was 84.6% on PVDF and 36.1% on ePAN, whereas the lyocell membrane had a lower degree of fouling at 30.6%. Lyocell membranes compare favorably regarding cake layer formation and fouling resistance for wastewater reclamation.

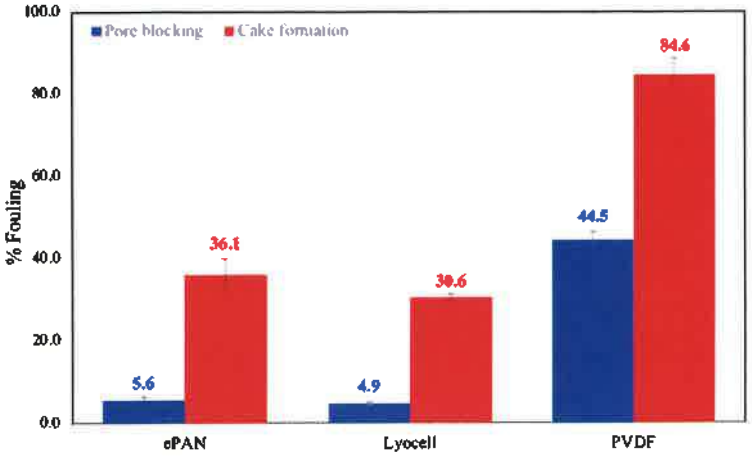

Figure 15. Computationally derived mechanisms of fouling: pore blocking and cake formation. From a Jupyter Notebook, ePAN, lyocell and PVDF flux values were inputted.

Turbidity, to measure permeate quality, was determined for CNF coated ePAN, CNF coated lyocell, and PVDF (Figure 16). The wastewater sample had a turbidity of 6.20 Nephelometric Turbidity Units (NTU). The lyocell membrane's low turbidity (0.41 NTU) indicate its feasibility in producing potable water since government regulations deem 0.5 and below NTU to be safe. Thus, lyocell's superior permeate quality demonstrate its potential to provide reclaimed wastewater.

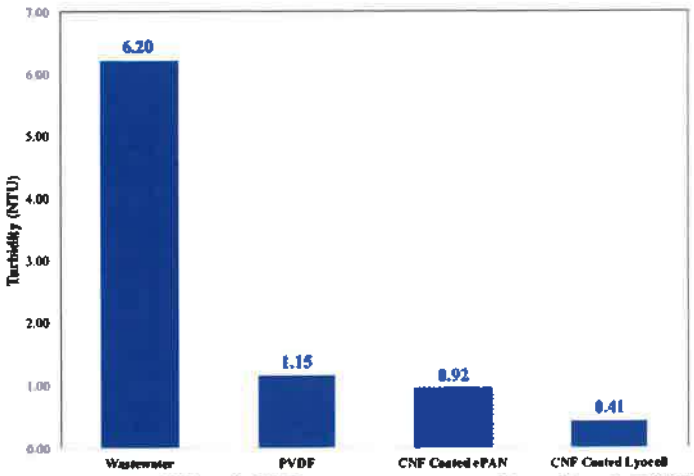

Figure 16. Turbidity of CNF coated ePAN and Lyocell and PVDF Membranes. Lyocell membrane's low turbidity indicate superior permeate quality compared to ePAN.

All-Cellulose Membrane

The all-cellulose lyocell-CNF mixture membrane had a remarkable flux recovery of 96% (Fig 17). However, a chemical treatment with sodium hypochlorite was required to maintain a high flux. Despite this limitation, the all-cellulose membrane exhibits great promise a high-flux fouling-resistant sustainable membrane for wastewater reclamation.

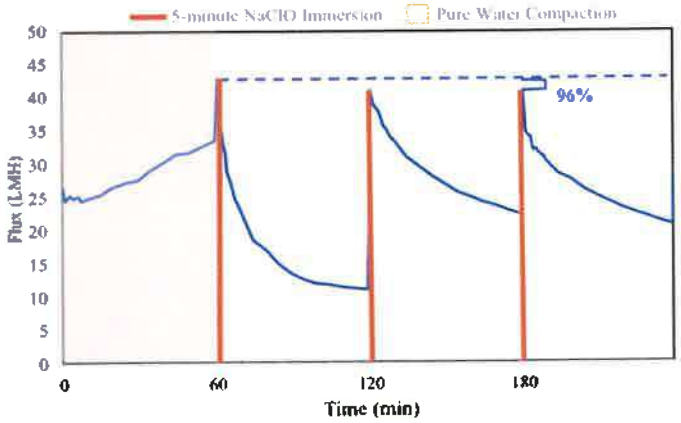

Figure 17. Dead-end Filtration of All-Cellulose Lyocell and CNF mixture Membrane.

CNF coated ePAN and lyocell membranes used in this study were compared to known characteristics of commercialized ultrafiltration membranes, PVDF, PAN, and PES (Table 1).

Table 1. ePAN and Lyocell Membranes compared to PVDF, PAN, and PES. Differences in Flux, Flux Recovery, Cake Formation, Cost, Production Time, Structure, Hydrophilicity/DO and AD.

	Polyvinylidene Difluoride A6	Polyacrylonitrile PX	Polyether Sulfone LX	Composite CNF coated ePAN	Composite CNF coated Lyocell	All-Cellulose Lyocell-CNF
Flux (LMH)	10-15	5-10	0-5	35-40	20-30	40-45
Flux Recovery	40%	29%	13%	98%	100%	96%
Cost	$26	$23	$27	$18	$5	$5
Production Time	-	-	-	18 hours	6 hours	18 hours
Structure	1 Layer: PVDF	1 Layer: PAN	1 Layer: PES	3 Layers (PET, ePAN, CNF)	3 Layers (PET, Lyocell, CNF)	Lyocell-CNF homogenous mixture
Hydrophilicity	Hydrophobic	Hydrophobic	Hydrophobic	Hydrophilic	Hydrophilic	Hydrophilic
AD	-	-	-	0.40AD	0.40AD	-

Both ePAN and lyocell membranes compare favorably regarding flux, flux recovery, and cost. These enhanced filtration properties can be attributed to composite structure and hydrophilicity (improved through increased CNF thicknesses and surface charges) of ePAN and lyocell membranes.

CONCLUSION

The development of inexpensive and efficient antifouling membranes is crucial to maximize ultrafiltration membrane efficiency for wastewater reclamation [90-92]. In this study, fouling resistance of TEMPO-oxidized CNF coated ePAN and lyocell scaffolds were investigated. Antifouling properties and membrane performance of CNF coated ePAN were evaluated using

CNF- layer thickness and surface charge density. Both CNF thickness and surface charge are vital in supporting the need for increased hydrophilicity and repulsions between wastewater foulants and the membrane, thus decreasing fouling. CNF coated ePAN membranes' permeability can be attributed to the high porosity of the ePAN scaffold [93, 94], and the fouling resistance was a result of CNF hydrophilicity. Current ultrafiltration wastewater treatment with ePAN can be adjusted according to these remarkable membrane enhancements to decrease operating costs, increase membrane lifetime and improve membrane efficiency [95].

The previously unstudied CNF coated lyocell membrane has outstanding potential to increase flux recovery and reduce fouling for wastewater membranes. Computational findings of Hermia's fouling models highlighted minimal caking on the lyocell membrane in comparison to ePAN suggesting superior fouling-resistance. The preliminary findings of fouling resistance of CNF coated lyocell membranes illustrate great promise because of its notable antifouling and economic and environmental benefits. Herein, an avenue for next-generation all-natural and all-cellulose wastewater ultrafiltration membranes was illuminated for the progression towards sustainable and affordable clean water for developing nations.

Lyocell membranes have the potential to cut current membrane costs by a factor of ten because of abundance and environmental preferability. However, to make CNF coated lyocell an industrial-grade membrane, further investigation is warranted to commercialize and industrialize its synthesis process and usage. Enhancement of lyocell's flux also requires further inquiry on techniques to improve permeate flux. Other future investigations should include studying CNF coated ePAN and lyocell membrane's antifouling characteristics in a crossflow system as crossflow modules are used in an industrial setting and have reported decreasing fouling [96-98]. Finally, investigating methods to maintain a high flux with the all-cellulose lyocell-CNF mixture membrane without chemical cleaning is required to develop a truly sustainable membrane [99-101].

Improvements in antifouling properties of current polymeric membranes and the introduction of lyocell as an exciting alternative ultrafiltration membrane scaffold are critical steps in determining efficient membrane operation for wastewater reclamation and identifying a viable solution to the global clean water scarcity.

References

[1] "Why Water? The Water Crisis in Africa," *The Water Project*. [Online]. Available: https://thewaterproject.org/why-water/water-crisis. [Accessed: 16-Sep-2019].
[2] UNICEF, *Progress on drinking water and sanitation: 2014 update*. Geneva: World Health Organization, UNICEF, 2014.
[3] X. Zheng, Z. Zhang, D. Yu, X. Chen, R. Cheng, S. Min, J. Wang, Q. Xiao, and J. Wang, "Overview of membrane technology applications for industrial wastewater treatment in China to increase water supply," *Resources, Conservation and Recycling*, vol. 105, pp. 1–10, 2015.
[4] S. Nair, B. George, H. M. Malano, M. Arora, and B. Nawarathna, "Water–energy–greenhouse gas nexus of urban water systems: Review of concepts, state-of-art and methods," *Resources, Conservation and Recycling*, vol. 89, pp. 1–10, 2014.
[5] C. Y. Tang, Z. Yang, H. Guo, J. J. Wen, L. D. Nghiem, and E. Cornelissen, "Potable Water Reuse through Advanced Membrane Technology," *Environmental Science & Technology*, vol. 52, no. 18, pp. 10215–10223, 2018.
[6] Z. Zhang and J. W. Balay, "How Much is Too Much?: Challenges to Water Withdrawal and Consumptive Use Management," *Journal of Water Resources Planning and Management*, vol. 140, no. 6, p. 01814001, 2014.
[7] K. Xiao, Y. Xu, S. Liang, T. Lei, J. Sun, X. Wen, H. Zhang, C. Chen, and X. Huang, "Engineering application of membrane bioreactor for wastewater treatment in China: Current state and future prospect," *Frontiers of Environmental Science & Engineering*, vol. 8, no. 6, pp. 805–819, Aug. 2014.
[8] K. Xiao, Y. Xu, S. Liang, T. Lei, J. Sun, X. Wen, H. Zhang, C. Chen, and X. Huang, "Engineering application of membrane bioreactor for wastewater treatment in China: Current state and future prospect," *Frontiers of Environmental Science & Engineering*, vol. 8, no. 6, pp. 805–819, Aug. 2014.
[9] R. Nazari, S. Eslamian, and R. Khanbilvardi, "Water Reuse and Sustainability," *Ecological Water Quality - Water Treatment and Reuse*, 2012.
[10] P. Roccaro, "Treatment processes for municipal wastewater reclamation: The challenges of emerging contaminants and direct potable reuse," *Current Opinion in Environmental Science & Health*, vol. 2, pp. 46–54, 2018.
[11] M. Gündoğdu, Y. A. Jarma, N. Kabay, T. Ö. Pek, and M. Yüksel, "Integration of MBR with NF/RO processes for industrial wastewater reclamation and water reuse-effect of membrane type on product water quality," *Journal of Water Process Engineering*, vol. 29, p. 100574, 2019.
[12] D. Dolar, M. Racar, and K. Košutić, "Municipal Wastewater Reclamation and Water Reuse for Irrigation by Membrane Processes," *Chemical and Biochemical Engineering Quarterly*, no. 3, Apr. 2019.
[13] S. M. Sadr and D. P. Saroj, "Membrane technologies for municipal wastewater treatment," *Advances in Membrane Technologies for Water Treatment*, pp. 443–463, 2015.
[14] B. A. Getachew, S.-R. Kim, and J.-H. Kim, "Self-Healing Hydrogel Pore-Filled Water Filtration Membranes," *Environmental Science & Technology*, vol. 51, no. 2, pp. 905–913, Jun. 2017.
[15] X. Li, L. Jiang, and H. Li, "Application of Ultrafiltration Technology in Water Treatment," *IOP Conference Series: Earth and Environmental Science*, vol. 186, p. 012009, Nov. 2018.
[16] M. Aslam, A. Charfi, G. Lesage, M. Heran, and J. Kim, "Membrane bioreactors for wastewater treatment: A review of mechanical cleaning by scouring agents to control membrane fouling," *Chemical Engineering Journal*, vol. 307, pp. 897–913, 2017.
[17] X. Li, L. Jiang, and H. Li, "Application of Ultrafiltration Technology in Water Treatment," *IOP Conference Series: Earth and Environmental Science*, vol. 186, p. 012009, Nov. 2018.
[18] G. Fan, Z. Su, R. Lin, X. Lin, R. Xu, and W. Chen, "Influence of Membrane Materials and Operational Modes on the Performance of Ultrafiltration Modules for Drinking Water Treatment," *International Journal of Polymer Science*, vol. 2016, pp. 1–8, 2016.
[19] D. S. Lakshmi, S. Jaiswar, M. Saxena, F. Tasselli, and H. D. Raval, "Preparation and performance of biofouling resistant PAN/chitosan hollow fiber membranes," *3 Biotech*, vol. 7, no. 3, 2017.
[20] P. Bahmani, A. Maleki, H. Daraei, M. Khamforoush, R. Rezaee, F. Gharibi, A. G. Tkachev, A. E. Burakov, S. Agarwal, and V. K. Gupta, "High-flux ultrafiltration membrane based on electrospun

polyacrylonitrile nanofibrous scaffolds for arsenate removal from aqueous solutions," *Journal of Colloid and Interface Science*, vol. 506, pp. 564–571, 2017.
[21] S. Talebian, A. M. Afifi, and H. M. Khanlou, "Fabrication and characterization of chitosan/polyvinyl alcohol nanofibres via electrospinning," *Materials Research Innovations*, vol. 18, no. sup6, May 2014.
[22] Y. Liu, R. Wang, H. Ma, B. S. Hsiao, and B. Chu, "High-flux microfiltration filters based on electrospun polyvinylalcohol nanofibrous membranes," *Polymer*, vol. 54, no. 2, pp. 548–556, 2013.
[23] D. Hou, Z. Wang, K. Wang, J. Wang, and S. Lin, "Composite membrane with electrospun multiscale-textured surface for robust oil-fouling resistance in membrane distillation," *Journal of Membrane Science*, vol. 546, pp. 179–187, 2018.
[24] M. Faccini, G. Borja, M. Boerrigter, D. M. Martin, S. M. Crespiera, S. Vázquez-Campos, L. Aubouy, and D. Amantia, "Electrospun Carbon Nanofiber Membranes for Filtration of Nanoparticles from Water," *Journal of Nanomaterials*, vol. 2015, pp. 1–9, 2015.
[25] X. Zhang, S. Yang, B. Yu, Q. Tan, X. Zhang, and H. Cong, "Advanced Modified Polyacrylonitrile Membrane with Enhanced Adsorption Property for Heavy Metal Ions," *Scientific Reports*, vol. 8, no. 1, 2018.
[26] G. M. Tolba, A. Bastaweesy, E. Ashour, W. Abdelmoez, K. A. Khalil, and N. A. Barakat, "Effective and highly recyclable ceramic membrane based on amorphous nanosilica for dye removal from the aqueous solutions," *Arabian Journal of Chemistry*, vol. 9, no. 2, pp. 287–296, 2016.
[27] W. Guo, H.-H. Ngo, and J. Li, "A mini-review on membrane fouling," *Bioresource Technology*, vol. 122, pp. 27–34, 2012.
[28] Y.-Y. Zhao, X.-M. Wang, H.-W. Yang, and Y.-F. F. Xie, "Effects of organic fouling and cleaning on the retention of pharmaceutically active compounds by ceramic nanofiltration membranes," *Journal of Membrane Science*, vol. 563, pp. 734–742, 2018.
[29] R. Rahmawati, M. Bilad, and N. Nordin, "Advanced Aeration Using Finned Panel Spacer For Fouling Control In Produced Water Membrane Filtration," *IOP Conference Series: Materials Science and Engineering*, vol. 429, p. 012022, Sep. 2018.
[30] X. Bao, Q. Wu, W. Shi, W. Wang, Z. Zhu, Z. Zhang, R. Zhang, X. Zhang, B. Zhang, Y. Guo, and F. Cui, "Insights into simultaneous ammonia-selective and anti-fouling mechanism over forward osmosis membrane for resource recovery from domestic wastewater," *Journal of Membrane Science*, vol. 573, pp. 135–144, 2019.
[31] J. Ochando-Pulido, V. Verardo, A. Segura-Carretero, and A. Martinez-Ferez, "Technical optimization of an integrated UF/NF pilot plant for conjoint batch treatment of two-phase olives and olive oil washing wastewaters," *Desalination*, vol. 364, pp. 82–89, 2015.[30] D. Lu, T. Zhang, L. Gutierrez, J.
[32] Jepsen, Kasper, et al. "Membrane Fouling for Produced Water Treatment: A Review Study From a Process Control Perspective." *Water*, vol. 10, no. 7, 2018, p. 847., doi:10.3390/w10070847.
[33] W. Zhang and B. Dong, "Effects of physical and chemical aspects on membrane fouling and cleaning using interfacial free energy analysis in forward osmosis," *Environmental Science and Pollution Research*, vol. 25, no. 22, pp. 21555–21567, 2018.
[34] M. N. Chollom and S. Rathilal, "Fouling and Cleaning in Osmotically Driven Membranes," *Osmotically Driven Membrane Processes - Approach, Development and Current Status*, 2018.
[35] J. Ochando-Pulido, V. Verardo, A. Segura-Carretero, and A. Martinez-Ferez, "Technical optimization of an integrated UF/NF pilot plant for conjoint batch treatment of two-phase olives and olive oil washing wastewaters," *Desalination*, vol. 364, pp. 82–89, 2015.[30] D. Lu, T. Zhang, L. Gutierrez, J.
[36] V. Kochkodan and N. Hilal, "A comprehensive review on surface modified polymer membranes for biofouling mitigation," *Desalination*, vol. 356, pp. 187–207, 2015.
[37] A. Halim, Y. Xu, K.-H. Lin, M. Kobayashi, M. Kajiyama, and T. Enomae, "Fabrication of cellulose nanofiber-deposited cellulose sponge as an oil-water separation membrane," *Separation and Purification Technology*, vol. 224, pp. 322–331, 2019.

[38] J. Teng, L. Shen, Y. He, B.-Q. Liao, G. Wu, and H. Lin, "Novel insights into membrane fouling in a membrane bioreactor: Elucidating interfacial interactions with real membrane surface," *Chemosphere*, vol. 210, pp. 769–778, 2018.
[39] C.-Y. Chong, W.-J. Lau, N. Yusof, G.-S. Lai, and A. F. Ismail, "Roles of nanomaterial structure and surface coating on thin film nanocomposite membranes for enhanced desalination," *Composites Part B: Engineering*, vol. 160, pp. 471–479, 2019.
[40] D. Wandera, H. H. Himstedt, M. Marroquin, S. R. Wickramasinghe, and S. M. Husson, "Modification of ultrafiltration membranes with block copolymer nanolayers for produced water treatment: The roles of polymer chain density and polymerization time on performance," *Journal of Membrane Science*, vol. 403-404, pp. 250–260, 2012.
[41] A. Ouradi, Q. Nguyen, and A. Benaboura, "Polysulfone–AN69 blend membranes and its surface modification by polyelectrolyte-layer deposit—Preparation and characterization," *Journal of Membrane Science*, vol. 454, pp. 20–35, 2014.
[42] D. Wandera and S. M. Husson, "Assessment of fouling-resistant membranes for additive-free treatment of high-strength wastewaters," *Desalination*, vol. 309, pp. 222–230, 2013.
[43] F. Gao, J. Wang, H. Zhang, H. Jia, Z. Cui, and G. Yang, "Aged PVDF and PSF ultrafiltration membranes restored by functional polydopamine for adjustable pore sizes and fouling control," *Journal of Membrane Science*, vol. 570-571, pp. 156–167, 2019.
[44] K. R. Kull, M. L. Steen, and E. R. Fisher, "Surface modification with nitrogen-containing plasmas to produce hydrophilic, low-fouling membranes," *Journal of Membrane Science*, vol. 246, no. 2, pp. 203–215, 2005.
[45] L. Zou, I. Vidalis, D. Steele, A. Michelmore, S. Low, and J. Verberk, "Surface hydrophilic modification of RO membranes by plasma polymerization for low organic fouling," *Journal of Membrane Science*, vol. 369, no. 1-2, pp. 420–428, 2011.
[46] Q. Li, X. Pan, C. Hou, Y. Jin, H. Dai, H. Wang, X. Zhao, and X. Liu, "Exploring the dependence of bulk properties on surface chemistries and microstructures of commercially composite RO membranes by novel characterization approaches," *Desalination*, vol. 292, pp. 9–18, 2012.
[47] H. Wu, X.-L. Chen, X. Huang, H.-M. Ruan, Y.-L. Ji, L.-F. Liu, and C.-J. Gao, "A novel semi-aromatic polyamide TFC reverse osmosis membrane fabricated from a dendritic molecule of trimesoylamidoamine through a two-step amine-immersion mode," *RSC Advances*, vol. 7, no. 62, pp. 39127–39137, 2017.
[48] N. Hilal, O. O. Ogunbiyi, N. J. Miles, and R. Nigmatullin, "Methods Employed for Control of Fouling in MF and UF Membranes: A Comprehensive Review," *Separation Science and Technology*, vol. 40, no. 10, pp. 1957–2005, 2005.
[49] V. Freger, J. Gilron, and S. Belfer, "TFC polyamide membranes modified by grafting of hydrophilic polymers: an FT-IR/AFM/TEM study," *Journal of Membrane Science*, vol. 209, no. 1, pp. 283–292, 2002.
[50] A. Isogai, T. Saito, and H. Fukuzumi, "TEMPO-oxidized cellulose nanofibers," *Nanoscale*, vol. 3, no. 1, pp. 71–85, 2011.
[51] L. Kong, D. Zhang, Z. Shao, B. Han, Y. Lv, K. Gao, and X. Peng, "Superior effect of TEMPO-oxidized cellulose nanofibrils (TOCNs) on the performance of cellulose triacetate (CTA) ultrafiltration membrane," *Desalination*, vol. 332, no. 1, pp. 117–125, 2014.
[52] S.-S. Shen, H. Chen, R.-H. Wang, W. Ji, Y. Zhang, and R. Bai, "Preparation of antifouling cellulose acetate membranes with good hydrophilic and oleophobic surface properties," *Materials Letters*, vol. 252, pp. 1–4, 2019.
[53] C. Ao, W. Yuan, J. Zhao, X. He, X. Zhang, Q. Li, T. Xia, W. Zhang, and C. Lu, "Superhydrophilic graphene oxide@electrospun cellulose nanofiber hybrid membrane for high-efficiency oil/water separation," *Carbohydrate Polymers*, vol. 175, pp. 216–222, 2017.
[54] F. Yalcinkaya, A. Siekierka, and M. Bryjak, "Surface modification of electrospun nanofibrous membranes for oily wastewater separation," *RSC Advances*, vol. 7, no. 89, pp. 56704–56712, 2017.

[55] Z. Xu, X. Li, K. Teng, B. Zhou, M. Ma, M. Shan, K. Jiao, X. Qian, and J. Fan, "High flux and rejection of hierarchical composite membranes based on carbon nanotube network and ultrathin electrospun nanofibrous layer for dye removal," *Journal of Membrane Science*, vol. 535, pp. 94–102, 2017.
[56] G.-R. Xu, X.-Y. Liu, J.-M. Xu, L. Li, H.-C. Su, H.-L. Zhao, and H.-J. Feng, "High flux nanofiltration membranes based on layer-by-layer assembly modified electrospun nanofibrous substrate," *Applied Surface Science*, vol. 434, pp. 573–581, 2018.
[57] M. Tang, D. Hou, C. Ding, K. Wang, D. Wang, and J. Wang, "Anti-oil-fouling hydrophobic-superoleophobic composite membranes for robust membrane distillation performance," *Science of The Total Environment*, vol. 696, p. 133883, 2019.
[58] J. Saththasivam, W. Yiming, K. Wang, J. Jin, and Z. Liu, "A Novel Architecture for Carbon Nanotube Membranes towards Fast and Efficient Oil/water Separation," *Scientific Reports*, vol. 8, no. 1, Sep. 2018.
[57] Y.-F. Guan, B.-C. Huang, Y.-J. Wang, B. Gong, X. Lu, and H.-Q. Yu, "Modification of forward osmosis membrane with naturally-available humic acid: Towards simultaneously improved filtration performance and antifouling properties," *Environment International*, vol. 131, p. 105045, 2019.
[60] S. Murad and L. C. Nitsche, "The effect of thickness, pore size and structure of a nanomembrane on the flux and selectivity in reverse osmosis separations: a molecular dynamics study," *Chemical Physics Letters*, vol. 397, no. 1-3, pp. 211–215, 2004.
[61] Y. Zhao, M. Zhang, and Z. Wang, "Underwater Superoleophobic Membrane with Enhanced Oil-Water Separation, Antimicrobial, and Antifouling Activities," *Advanced Materials Interfaces*, vol. 3, no. 13, p. 1500664, 2016.
[62] Z. Anari, A. Sengupta, K. Sardari, and S. R. Wickramasinghe, "Surface modification of PVDF membranes for treating produced waters by direct contact membrane distillation," *Separation and Purification Technology*, vol. 224, pp. 388–396, 2019.
[63] L. Geng, A. Naderi, Y. Mao, C. Zhan, P. Sharma, X. Peng, and B. S. Hsiao, "Rheological Properties of Jute-Based Cellulose Nanofibers under Different Ionic Conditions," *Nanocelluloses: Their Preparation, Properties, and Applications ACS Symposium Series*, pp. 113–132, 2017
[64] A. Ismail, M. Padaki, N. Hilal, T. Matsuura, and W. Lau, "Thin film composite membrane — Recent development and future potential," *Desalination*, vol. 356, pp. 140–148, 2015.
[65]W. Gindl and J. Keckes, "Tensile properties of cellulose acetate butyrate composites reinforced with bacterial cellulose," *Composites Science and Technology*, vol. 64, no. 15, pp. 2407–2413, 2004.
[66] E. Borbély, "Lyocell, The New Generation of Regenerated Cellulose ," *Acta Polytechnica Hungarica* , vol. 5, no. 3, 2008.
[67]K. E. Perepelkin, "Lyocell fibres based on direct dissolution of cellulose in N-methylmorpholine N-oxide: Development and prospects," *Fibre Chemistry*, vol. 39, no. 2, pp. 163–172, 2007.
[68] P. Hadi, M. Yang, H. Ma, X. Huang, H. Walker, and B. S. Hsiao, "Biofouling-resistant nanocellulose layer in hierarchical polymeric membranes: Synthesis, characterization and performance," *Journal of Membrane Science*, vol. 579, pp. 162–171, 2019.
[69] E.-E. Chang, S.-Y. Yang, C.-P. Huang, C.-H. Liang, and P.-C. Chiang, "Assessing the fouling mechanisms of high-pressure nanofiltration membrane using the modified Hermia model and the resistance-in-series model," *Separation and Purification Technology*, vol. 79, no. 3, pp. 329–336, 2011.
[70] M. C. V. Vela, S. Á. Blanco, J. L. García, and E. B. Rodríguez, "Analysis of membrane pore blocking models adapted to crossflow ultrafiltration in the ultrafiltration of PEG," *Chemical Engineering Journal*, vol. 149, no. 1-3, pp. 232–241, Jan. 2009.
[71] F. Wang and V. V. Tarabara, "Pore blocking mechanisms during early stages of membrane fouling by colloids," *Journal of Colloid and Interface Science*, vol. 328, no. 2, pp. 464–469, 2008.
[72] M. A. Indok Nurul Hasyimah and A.W. Mohammad,"Assessment of Fouling Mechanisms in Treating Organic Solutes Synthesizing Glycerin–Water Solutions by Modified Hermia Model," *Industrial & Engineering Chemistry Research*, vol. 53, no. 39, pp. 15213–15221, 2014.

[73] W. Zhang and F. Jiang, "Membrane fouling in aerobic granular sludge (AGS)-membrane bioreactor (MBR): Effect of AGS size," *Water Research*, vol. 157, pp. 445–453, 2019.
[74] J. Liu, C. Y. Eng, J. S. Ho, T. H. Chong, L. Wang, P. Zhang, and Y. Zhou, "Quorum quenching in anaerobic membrane bioreactor for fouling control," *Water Research*, vol. 156, pp. 159–167, 2019.
[75] F. Mashayekhi, H. Hazrati, and J. Shayegan, "Fouling control mechanism by optimum ozone addition in submerged membrane bioreactors treating synthetic wastewater," *Journal of Environmental Chemical Engineering*, vol. 6, no. 6, pp. 7294–7301, 2018.
[76] L. Deng, H.-H. Ngo, W. Guo, and H. Zhang, "Pre-coagulation coupled with sponge-membrane filtration for organic matter removal and membrane fouling control during drinking water treatment," *Water Research*, vol. 157, pp. 155–166, 2019.
[77] W. Yu, N. Graham, Y. Yang, Z. Zhou, and L. C. Campos, "Effect of sludge retention on UF membrane fouling: The significance of sludge crystallization and EPS increase," *Water Research*, vol. 83, pp. 319–328, 2015.
[78] Z. Yan, H. Yang, F. Qu, H. Zhang, H. Rong, H. Yu, H. Liang, A. Ding, G. Li, and B. V. D. Bruggen, "Application of membrane distillation to anaerobic digestion effluent treatment: Identifying culprits of membrane fouling and scaling," *Science of The Total Environment*, vol. 688, pp. 880–889, 2019.
[79] F.-M. Chang, S.-J. Hong, Y.-J. Sheng, and H.-K. Tsao, "High contact angle hysteresis of superhydrophobic surfaces: Hydrophobic defects," *Applied Physics Letters*, vol. 95, no. 6, p. 064102, Oct. 2009.
[80] K.-Y. Law, "Definitions for Hydrophilicity, Hydrophobicity, and Superhydrophobicity: Getting the Basics Right," *The Journal of Physical Chemistry Letters*, vol. 5, no. 4, pp. 686–688, 2014.
[81] M. Zhang, B.-Q. Liao, X. Zhou, Y. He, H. Hong, H. Lin, and J. Chen, "Effects of hydrophilicity/hydrophobicity of membrane on membrane fouling in a submerged membrane bioreactor," *Bioresource Technology*, vol. 175, pp. 59–67, 2015.
[82] S. Wang, X. Lu, L. Zhang, J. Guo, and H. Zhang, "Characterization of the Initial Fouling Layer on the Membrane Surface in a Membrane Bioreactor: Effects of Permeation Drag," *Membranes*, vol. 9, no. 9, p. 121, 2019.
[83] G. V. D. Staey, G. Gins, and I. Smets, "Bioflocculation and Activated Sludge Separation: A PLS Case Study," *IFAC-PapersOnLine*, vol. 49, no. 7, pp. 1151–1156, 2016.
[84] "Hydrophilic PVDF Membranes," Sterlitech Corporation. [Online]. Available: https://www.sterlitech.com/hydrophilic-pvdf-membranes.html. [Accessed: 27-Oct-2019].
[85] F. Yalcinkaya, B. Yalcinkaya, A. Pazourek, J. Mullerova, M. Stuchlik, and J. Maryska, "Surface Modification of Electrospun PVDF/PAN Nanofibrous Layers by Low Vacuum Plasma Treatment," International Journal of Polymer Science, vol. 2016, pp. 1–9, 2016.
[86] "Polyacrylonitrile Ultrafiltration Membranes (UF Membranes)," Polyacrylonitrile Ultrafiltration Membranes - UF PAN Membranes | Applied Membranes Inc. [Online]. Available: https://appliedmembranes.com/polyacrylonitrile-ultrafiltration-membranes-uf-membranes.html. [Accessed: 27-Oct-2019].
[87] N. A. Alenazi, M. A. Hussein, K. A. Alamry, and A. M. Asiri, "Modified polyether-sulfone membrane: a mini review," Designed Monomers and Polymers, vol. 20, no. 1, pp. 532–546, 2017.
[88] "Polyethersulfone Ultrafiltration Membranes (UF Membranes)," Polyethersulfone UF Membranes - PES Ultrafiltration Membrane | Applied Membranes Inc. [Online]. Available: https://appliedmembranes.com/polyethersulfone-ultrafiltration-membranes-uf- membranes.html. [Accessed: 27-Oct-2019].
[89] R. Roche and F. Yalcinkaya, "Electrospun Polyacrylonitrile Nanofibrous Membranes forPoint-of-Use Water and Air Cleaning," ChemistryOpen, vol. 8, no. 1, pp. 97–103, 2019.

[90] Zhang, Runnan, et al. "Antifouling Membranes for Sustainable Water Purification: Strategies and Mechanisms." *Chemical Society Reviews*, vol. 45, no. 21, 2016, pp. 5888–5924., doi:10.1039/c5cs00579e.

[91] Peña, N., et al. "Evaluating Impact of Fouling on Reverse Osmosis Membranes Performance." *Desalination and Water Treatment*, vol. 51, no. 4-6, 2013, pp. 958–968., doi:10.1080/19443994.2012.699509.
[92] Sun, Wen, et al. "Pretreatment and Membrane Hydrophilic Modification to Reduce Membrane Fouling." *Membranes*, vol. 3, no. 3, Apr. 2013, pp. 226–241., doi:10.3390/membranes3030226.
[93] N. Wang, K. Burugapalli, W. Song, J. Halls, F. Moussy, Y. Zheng, Y. Ma, Z. Wu, and K. Li, "Tailored fibro-porous structure of electrospun polyurethane membranes, their size-dependent properties and trans-membrane glucose diffusion," *Journal of Membrane Science*, vol. 427, pp. 207–217, 2013.
[94] Y. Bagbi, A. Pandey, and P. R. Solanki, "Electrospun Nanofibrous Filtration Membranes for Heavy Metals and Dye Removal," *Nanoscale Materials in Water Purification*, pp. 275–288, 2019.
[95] Huang, Shilin, et al. "Antifouling Membranes for Oily Wastewater Treatment: Interplay between Wetting and Membrane Fouling." *Current Opinion in Colloid & Interface Science*, vol. 36, 2018, pp. 90–109., doi:10.1016/j.cocis.2018.02.002.
[96] Ilias, Shamsuddin. "Flux Enhancement in Crossflow Membrane Filtration: Fouling and Its Minimization by Flow Reversal." Apr. 2005, doi:10.2172/859173.
[97] Miller, Daniel J., et al. "A Crossflow Filtration System for Constant Permeate Flux Membrane Fouling Characterization." *Review of Scientific Instruments*, vol. 84, no. 3, 2013, p. 035003., doi:10.1063/1.4794909.
[98] I. Hassan, M. Ennouri, C. Lafforgue, P. Schmitz, and A. Ayadi, "Experimental Study of Membrane Fouling during Crossflow Microfiltration of Yeast and Bacteria Suspensions: Towards an Analysis at the Microscopic Level," *Membranes*, vol. 3, no. 2, pp. 44–68, Oct. 2013.
[99] H. Chang, T. Li, B. Liu, C. Chen, Q. He, and J. C. Crittenden, "Smart ultrafiltration membrane fouling control as desalination pretreatment of shale gas fracturing wastewater: The effects of backwash water," *Environment International*, vol. 130, p. 104869, 2019.
[100] A. Ignatev and T. Tuhkanen, "Step-by-step analysis of drinking water treatment trains using size-exclusion chromatography to fingerprint and track protein-like and humic/fulvic-like fractions of dissolved organic matter," *Environmental Science: Water Research & Technology*, vol. 5, no. 9, pp. 1568–1581, 2019.
[101] E. N. Hidayah and O. H. Cahyonugroho, "Tracking of Dissolved Effluent Organic Matter (dEfOM) in wastewater treatment plant by using fluorescence method," *IOP Conference Series: Earth and Environmental Science*, vol. 245, p. 012018, 2019.